Efficient and accurate numerical simulation of acoustic wave propagation in a 2D heterogeneous media

Wenyuan Liao [a,*], Peng Yong [a,b], Hatef Dastour [a], Jianping Huang [b]

[a] *Department of Mathematics & Statistics, University of Calgary, AB, T2N 1N4, Canada*
[b] *School of Geosciences, China University of Petroleum, Qingdao 266580, China*

A B S T R A C T

In this paper, a compact fourth-order finite difference scheme is derived to solve the 2D acoustic wave equation in heterogenous media. The Padé approximation is used to obtain fourth-order accuracy in both temporal and spatial dimensions, and the alternating direction implicit (ADI) technique is used to reduce the computational cost. Due to the non-constant wave velocity, the conventional ADI method is hard to implement as the algebraic manipulation cannot be used here. A novel numerical strategy is proposed in this work so that the compact scheme still maintains fourth-order accuracy in time and space. The fourth-order convergence order was firstly proved by theoretical error analysis, then was confirmed by numerical examples. It was shown that the proposed method is conditionally stable with a Courant–Friedrichs–Lewy (CFL) condition that is comparable to other existing finite difference schemes. Several numerical examples were solved to demonstrate the efficiency and accuracy of the new algorithm.

© 2017 Elsevier Inc. All rights reserved.

1. Introduction

Finite difference (FD) method is one of the powerful numerical approaches that has been used in various science and engineering applications where the analytical solution is not available. One such example is the numerical modeling of seismic wave propagation, as the closed-form analytical solution of a seismic wave equation is usually not available. In particular, the higher-order FD methods have attracted the interests of many researchers working on seismic modeling (see [2,4,10,14,19–21,25,27,28] and references therein) due to the higher-order accuracy and effectiveness in suppressing numerical dispersion.

Recently, a great deal of efforts have been devoted to develop higher-order FD schemes for the acoustic equations, and many accurate and efficient methods haven been reported. Levander [13] addressed the cost-effectiveness of solving real problems using higher-order spatial derivatives to allow a more coarse spatial sample rate. In [19], the authors used a plane wave theory and the Taylor series expansion to develop a low dispersive time-space domain FD scheme with error of $O(\Delta t^2 + h^{2M})$ for 1-D, 2-D and 3-D acoustic wave equations, where Δt and h represent the time step and spatial grid size, respectively. It was then shown that, along certain fixed directions the error can be improved to $O(\Delta t^{2M} + h^{2M})$. In [4], Cohen and Poly extended the works of Dablain [5], Shubin and Bell [23] and Bayliss et al. [1] and developed a fourth-order accurate explicit scheme with error of $O(\Delta t^4 + h^4)$ to solve the heterogeneous acoustic wave equation. Moreover, it has

been reported that highly accurate numerical methods are very effective in suppressing the annoying numerical dispersion [9,29,31].

These methods are accurate but are non-compact, which gives rise to two issues: efficiency and difficulty in boundary condition treatment. For example, a non-compact fourth-order FD scheme requires a five-point stencil in 1D and 9-point stencil in 2D to approximate the derivative u_{xx} and $\triangle u$, respectively. To resolve these issues, a variety of compact higher-order FD schemes to approximate the spatial derivatives have been developed. In [3], the authors developed a family of fourth-order three-point combined difference schemes to approximate the first- and second-order spatial derivatives. In [11], the authors introduced a family of three-level implicit FD schemes which incorporate the locally one-dimensional method. For more recent compact higher-order difference methods, the readers are referred to [14,24,26].

On the other hand, it is well-known that for multi-dimensional problems, a block tridiagonal system needs to be solved at each time step for implicit method. To efficiently solve such large linear system, some operator splitting techniques are usually used to convert the multi-dimensional problem into a sequence of one-dimensional problems. One such operator splitting method is the alternating direction implicit (ADI) method, which was originally introduced by Peaceman and Rachford [22] to solve parabolic and elliptic equations. Since then a lot of developments have been made over the years for hyperbolic equations as well [7,12]. For example, Fairweather and Mitchell [8] developed a fourth-order compact ADI scheme for solving the wave equation. Some other related work can be found in [15,16]. Combine with Padé approximation of the finite difference operator, some efficient and higher-order compact finite difference methods have been developed to solve the acoustic wave equations in 2D and 3D with constant velocity [6,18]. However, when the velocity is a spatially varying function, it is difficult to apply the same technique because the algebraic manipulation used in [6,18] is not applicable here.

Recently there were some research work on accurate and low-dispersive numerical simulation of acoustic wavefields in heterogeneous media [30–32]. However these methods are either non-compact or only focus on special case. For example a layered model consisting of multiple horizontal homogeneous layers was considered [32], in which the method development and stability analysis are based on constant velocity model.

In this paper, we introduce a novel operator splitting approach so that we can extend the Padé approximation based higher-order compact FD scheme in [6,18] to the 2D acoustic wave equation with non-constant velocity. The new method is compact and efficient, with fourth-order accuracy in both time and space. To our best knowledge, this is the first attempt to develop compact higher-order ADI method for solving acoustic wave equation in heterogeneous media. The rest of the paper is organized as the follows. We first give a brief introduction of the standard second-order central FD scheme, compact higher-order FD scheme for spatial derivatives and some other related higher-order method in Section 2, then derive the new compact fourth-order ADI FD scheme in Section 3, which is followed by the numerical stability analysis in Section 4. The accuracy and efficiency of the new method are demonstrated by several numerical examples in Section 5. Finally, the conclusions and possible future extensions are discussed in Section 6.

2. Review of finite difference schemes for acoustic wave equation

Consider the 2D acoustic wave equation

$$u_{tt} = v^2(x, y)(u_{xx} + u_{yy}) + s(x, y, t), \quad (x, y, t) \in \Omega \times [0, T], \tag{1}$$

which is supplemented with the initial conditions

$$u(x, y, 0) = f_1(x, y), \quad (x, y) \in \Omega, \tag{2}$$

$$u_t(x, y, 0) = f_2(x, y), \quad (x, y) \in \Omega \tag{3}$$

and the boundary condition

$$u(x, y, t) = g(x, y, t), \quad (x, y, t) \in \partial\Omega \times [0, T], \tag{4}$$

where $v(x, y)$ represents the wave velocity. Here, $\Omega \subset R^2$ is a finite computational domain and $s(x, y, t)$ is the source function. For the convenience of method derivation, let $c(x, y) = v^2(x, y)$.

For the sake of simplicity, we assume that Ω is a rectangular domain which will be discretized into an $N_x \times N_y$ grid with spatial grid sizes h_x and h_y. Let Δt denote the time step, $u_{i,j}^n$ denotes the numerical solution at the grid point (x_i, y_j) and time level $n\Delta t$. In the standard central FD scheme, all second derivatives in Eq. (1) are approximated by the following second-order central difference formulas:

$$u_{tt}(x_i, y_j, t_n) \approx \delta_t^2 u_{i,j}^n / \Delta t^2 = (u_{i,j}^{n-1} - 2u_{i,j}^n + u_{i,j}^{n+1}) / \Delta t^2, \tag{5}$$

$$u_{xx}(x_i, y_j, t_n) \approx \delta_x^2 u_{i,j}^n / h_x^2 = (u_{i-1,j}^n - 2u_{i,j}^n + u_{i+1,j}^n) / h_x^2, \tag{6}$$

$$u_{yy}(x_i, y_j, t_n) \approx \delta_y^2 u_{i,j}^n / h_y^2 = (u_{i,j-1}^n - 2u_{i,j}^n + u_{i,j+1}^n) / h_y^2. \tag{7}$$

To obtain higher-order scheme, one needs to approximate these derivatives with higher-order accuracy. The conventional higher-order FD method was derived by approximating the spatial derivatives using more than three points in one direction, which results in large stencil. For instance, if $2M + 1$ points are used to approximate u_{xx}, one obtains the following formula:

$$u_{xx}(x_i, y_j, t_n) \approx \frac{1}{h_x^2}\left[a_0 u_{i,j}^n + \sum_{m=1}^{M} a_m (u_{i-m,j}^n + u_{i+m,j}^n) \right], \tag{8}$$

which can be as accurate as $(2M)$th-order in space. The conventional high-order FD method is accurate in space but suffers severe numerical dispersion. Another issue is that it requires more computer memory due to the larger stencil for implicit method. Moreover, more points are needed near the boundary.

To improve the accuracy in time, a class of time-domain high-order FD methods have been derived by Liu and Sen [19,20]. The idea of the time-domain high-order FD method is to determine coefficients using time-space domain dispersion. As a result, the coefficient a_m will be a function of the ratio $\frac{v\Delta t}{h}$. It was noted that in 1D case, the time-domain high-order FD method can be as accurate as $(2M)$th-order in both time and space, provided some conditions are satisfied. For multi-dimensional case, $(2M)$th-order is also possible along some propagation directions.

To obtain higher-order compact ADI FD scheme, we can apply Padé approximation to the second-order central FD operators defined in Eqs. (5)–(7). The Padé approximation is a technique originally developed to approximate a generic function by a rational one. Simply speaking, if $r > 0$ is a small perturbation, the function $1 - r$ can be approximated by $\frac{1}{1+r}$ with a higher-order error $O(r^2)$. It is known that the second-order central difference operator δ_x^2 approximates u_{xx} with second-order accuracy. Moreover, Taylor series analysis shows that

$$\frac{1}{h_x^2}\delta_x^2 u_{i,j}^n - \frac{h_x^2}{12}\delta_x^2 \delta_x^2 u_{i,j}^n = u_{xx}(x_i, y_j, t_n) + O(h_x^4). \tag{9}$$

Re-arranging the terms we obtain

$$u_{xx}(x_i, y_j, t_n) = \frac{1}{h_x^2}\delta_x^2\left(1 - \frac{1}{12}\delta_x^2\right)u_{i,j}^n + O(h_x^4). \tag{10}$$

Substituting the perturbation r in Padé approximation with the operator $\frac{1}{12}\delta_x^2$ leads to the following fourth-order compact approximation:

$$\frac{\delta_x^2}{h_x^2\left(1 + \frac{1}{12}\delta_x^2\right)}u_{i,j}^n = u_{xx}(x_i, y_j, t_n) + O(h_x^4). \tag{11}$$

Similarly, the second derivatives u_{yy} and u_{tt} are approximated with fourth-order accuracy in y and t, respectively

$$\frac{\delta_y^2}{h_y^2\left(1 + \frac{1}{12}\delta_y^2\right)}u_{i,j}^n = u_{yy}(x_i, y_j, t_n) + O(h_y^4), \tag{12}$$

$$\frac{\delta_t^2}{\Delta t^2\left(1 + \frac{1}{12}\delta_t^2\right)}u_{i,j}^n = u_{tt}(x_i, y_j, t_n) + O(\Delta t^4). \tag{13}$$

A detailed description of the Padé approximation of the second-order central finite difference operator can be found in [17].

Substituting the Padé approximations defined in Eqs. (11)–(13) into Eq. (1) yields

$$\frac{\delta_t^2}{(1 + \frac{1}{12}\delta_t^2)}u_{i,j}^n = c_{i,j}\left[\frac{\Delta t^2 \delta_x^2}{h_x^2(1 + \frac{1}{12}\delta_x^2)} + \frac{\Delta t^2 \delta_y^2}{h_y^2(1 + \frac{1}{12}\delta_y^2)} \right]u_{i,j}^n + \Delta t^2 s_{i,j}^n, \tag{14}$$

which is fourth-order accurate in time and space with the truncation error $O(\Delta t^4 + h_x^4 + h_y^4)$. When $c(x, y)$ is a constant, one can multiply the operator

$$\left(1 + \frac{1}{12}\delta_t^2\right)\left(1 + \frac{1}{12}\delta_x^2\right)\left(1 + \frac{1}{12}\delta_y^2\right) \tag{15}$$

to both sides of Eq. (14) to cancel the operators $(1 + \frac{1}{12}\delta_t^2)^{-1}$, $(1 + \frac{1}{12}\delta_x^2)^{-1}$ and $(1 + \frac{1}{12}\delta_y^2)^{-1}$. Then the original equation can be factorized and efficiently solved by ADI algorithm [6,18]. However it is difficult to utilize such algebraic manipulation when the velocity is non-constant, because the operator in Eq. (15) is not commutative with $c_{i,j}$.

In the next section, we introduce a novel approach to overcome this problem and obtain the fourth-order compact FD scheme, which still allows efficient ADI implementation of the algorithm.

3. The new compact higher-order ADI FD scheme

We first illustrate the difficulty in applying the traditional Padé approximation to the acoustic wave equation with non-constant velocity. Multiplying the operator in Eqs. (15) to (14) yields

$$
\left(1 + \frac{1}{12}\delta_x^2\right)\left(1 + \frac{1}{12}\delta_y^2\right)\delta_t^2 u_{i,j}^n = \frac{\Delta t^2}{h_x^2}\left(1 + \frac{1}{12}\delta_t^2\right)\left(1 + \frac{1}{12}\delta_x^2\right)\left(1 + \frac{1}{12}\delta_y^2\right)c_{i,j}\frac{\delta_x^2}{\left(1 + \frac{1}{12}\delta_x^2\right)}u_{i,j}^n
$$
$$
+ \frac{\Delta t^2}{h_y^2}\left(1 + \frac{1}{12}\delta_t^2\right)\left(1 + \frac{1}{12}\delta_x^2\right)\left(1 + \frac{1}{12}\delta_y^2\right)c_{i,j}\frac{\delta_y^2}{\left(1 + \frac{1}{12}\delta_y^2\right)}u_{i,j}^n
$$
$$
+ \Delta t^2\left(1 + \frac{1}{12}\delta_t^2\right)\left(1 + \frac{1}{12}\delta_x^2\right)\left(1 + \frac{1}{12}\delta_y^2\right)s_{i,j}^n. \tag{16}
$$

We use the first term on the right-hand side to demonstrate the difficulty here. Since $(1 + \frac{\delta_x^2}{12})$ and $(1 + \frac{\delta_y^2}{12})$ are commutative, we have

$$
\frac{\Delta t^2}{h_x^2}\left(1 + \frac{1}{12}\delta_t^2\right)\left(1 + \frac{1}{12}\delta_x^2\right)\left(1 + \frac{1}{12}\delta_y^2\right)c_{i,j}\frac{\delta_x^2}{\left(1 + \frac{1}{12}\delta_x^2\right)}u_{i,j}^n
$$
$$
= \frac{\Delta t^2}{h_x^2}\left(1 + \frac{1}{12}\delta_t^2\right)\left(1 + \frac{1}{12}\delta_y^2\right)\left(1 + \frac{1}{12}\delta_x^2\right)c_{i,j}\frac{\delta_x^2}{\left(1 + \frac{1}{12}\delta_x^2\right)}u_{i,j}^n. \tag{17}
$$

As discussed previously, when $c(x, y)$ is non-constant, the operator $(1 + \frac{1}{12}\delta_x^2)$ and $c_{i,j}$ are not commutative. Hence $\left(1 + \frac{1}{12}\delta_x^2\right)c_{i,j} \neq c_{i,j}\left(1 + \frac{1}{12}\delta_x^2\right)$. Therefore, the operator $\left(1 + \frac{1}{12}\delta_x^2\right)$ does not cancel the operator $\left(1 + \frac{1}{12}\delta_x^2\right)^{-1}$. In other words

$$
\frac{\Delta t^2}{h_x^2}\left(1 + \frac{1}{12}\delta_t^2\right)\left(1 + \frac{1}{12}\delta_y^2\right)\left(1 + \frac{1}{12}\delta_x^2\right)c_{i,j}\frac{\delta_x^2}{\left(1 + \frac{1}{12}\delta_x^2\right)}u_{i,j}^n \neq \frac{\Delta t^2}{h_x^2}\left(1 + \frac{1}{12}\delta_t^2\right)\left(1 + \frac{1}{12}\delta_y^2\right)c_{i,j}\ \delta_x^2 u_{i,j}^n. \tag{18}
$$

To solve this problem, a novel factorization technique is used to preserve the compactness of the numerical scheme, while still maintain fourth-order accuracy in space and time.

Let $\lambda_x = \frac{\Delta t^2}{h_x^2}$, $\lambda_y = \frac{\Delta t^2}{h_y^2}$. Multiplying $(1 + \frac{\delta_t^2}{12})$ to both sides of Eq. (14) yields

$$
\delta_t^2 u_{i,j}^n = c_{i,j}\left[\lambda_x\left(1 + \frac{\delta_t^2}{12}\right)\frac{\delta_x^2}{(1 + \frac{1}{12}\delta_x^2)} + \lambda_y\left(1 + \frac{\delta_t^2}{12}\right)\frac{\delta_y^2}{(1 + \frac{1}{12}\delta_y^2)}\right]u_{i,j}^n + \Delta t^2\left(1 + \frac{\delta_t^2}{12}\right)s_{i,j}^n. \tag{19}
$$

Collecting the term $\delta_t^2 u_{i,j}^n$ leads to

$$
\left[1 - \frac{\lambda_x c_{i,j}}{12}\frac{\delta_x^2}{(1 + \frac{1}{12}\delta_x^2)} - \frac{\lambda_y c_{i,j}}{12}\frac{\delta_y^2}{(1 + \frac{1}{12}\delta_y^2)}\right]\delta_t^2 u_{i,j}^n = c_{i,j}\left[\lambda_x\frac{\delta_x^2}{(1 + \frac{1}{12}\delta_x^2)} + \lambda_y\frac{\delta_y^2}{(1 + \frac{1}{12}\delta_y^2)}\right]u_{i,j}^n + \Delta t^2\left(1 + \frac{\delta_t^2}{12}\right)s_{i,j}^n. \tag{20}
$$

Factoring the left-hand side of Eq. (20) gives

$$
\left[1 - \frac{\lambda_x c_{i,j}}{12}\frac{\delta_x^2}{(1 + \frac{1}{12}\delta_x^2)}\right] \cdot \left[1 - \frac{\lambda_y c_{i,j}}{12}\frac{\delta_y^2}{(1 + \frac{1}{12}\delta_y^2)}\right]\delta_t^2 u_{i,j}^n
$$
$$
= c_{i,j}\left[\lambda_x\frac{\delta_x^2}{(1 + \frac{1}{12}\delta_x^2)} + \lambda_y\frac{\delta_y^2}{(1 + \frac{1}{12}\delta_y^2)}\right]u_{i,j}^n + \Delta t^2\left(1 + \frac{\delta_t^2}{12}\right)s_{i,j}^n + ERR, \tag{21}
$$

where the factorization error ERR is given by

$$
ERR = \frac{\lambda_x}{144}\ c_{i,j}\frac{\delta_x^2}{(1 + \frac{1}{12}\delta_x^2)}\ \lambda_y\ c_{i,j}\frac{\delta_y^2}{(1 + \frac{1}{12}\delta_y^2)}\delta_t^2 u_{i,j}^n. \tag{22}
$$

We now give the estimate of the truncation error, which will be used in the convergence analysis.

Theorem 3.1. *Assume that $u(x, y, t) \in C_{x,y,t}^{6,6,6}(\Omega \times [0, T])$ is the solution of the acoustic wave Eqs. (1)–(4), and the coefficient function satisfies the smooth condition $c(x, y) \in C_x^2(\Omega)$. Then the truncation error given in Eq. (22) satisfies*

$$
ERR = O(\Delta t^6).
$$

Proof. Expanding $\delta_t^2 u_{i,j}^n$ by Taylor series at time t_n, we have

$$
\delta_t^2 u_{i,j}^n = u_{i,j}^{n+1} - 2u_{i,j}^n + u_{i,j}^{n-1} = \Delta t^2 \frac{\partial^2 u}{\partial t^2}|_{i,j}^n + \frac{\Delta t^4}{12}\frac{\partial^4 u}{\partial t^4}|_{i,j}^n + \frac{\Delta t^6}{360}\frac{\partial^6 u(x_i, y_j, \tau_n)}{\partial t^6}, \tag{23}
$$

where $\tau_n \in (t_{n-1}, t_{n+1})$.

By Padé approximation, for any sufficiently smooth function $v(x, y, t)$,

$$\frac{\delta_y^2}{(1 + \frac{1}{12}\delta_y^2)} v_{i,j}^n = \delta_y^2 \left(1 - \frac{\delta_y^2}{12}\right) v_{i,j}^n + \frac{h_y^6}{144} \frac{\partial^6 v(x_i, \eta_j, t_n)}{\partial y^6}, \tag{24}$$

where $\eta_j \in (y_{j-1}, y_{j+1})$.

Letting $v_{i,j}^n = \delta_t^2 u_{i,j}^n$ in Eq. (24) leads to

$$\frac{\delta_y^2}{(1 + \frac{1}{12}\delta_y^2)} \delta_t^2 u_{i,j}^n = \delta_y^2 v_{i,j}^n - \frac{1}{12}\delta_y^2 \delta_y^2 v_{i,j}^n + \frac{h_y^6}{144} \frac{\partial^6 v(x_i, \eta_j, t_n)}{\partial y^6}$$

$$= \frac{1}{12}(-v_{i,j+2}^n + 16v_{i,j+1}^n - 30v_{i,j}^n + 16v_{i,j-1}^n - v_{i,j-2}^n) + \frac{h_y^6}{144} \frac{\partial^6 v(x_i, \eta_j, t_n)}{\partial y^6}. \tag{25}$$

Expanding it by Taylor series, we have

$$\frac{\delta_y^2}{(1 + \frac{1}{12}\delta_y^2)} \delta_t^2 u_{i,j}^n = h_y^2 \frac{\partial^2 v}{\partial y^2}\Big|_{i,j}^n - \frac{2}{15}h_y^6 \frac{\partial^6 v(x_i, \bar{\eta}_j, t_n)}{\partial y^6} + \frac{h_y^6}{144} \frac{\partial^6 v(x_i, \eta_j, t_n)}{\partial y^6}, \tag{26}$$

where $\bar{\eta}_j \in (y_{j-1}, y_{j+1})$. Combining Eqs. (23) and (26) yields

$$\lambda_y \, c_{i,j} \frac{\delta_y^2}{(1 + \frac{1}{12}\delta_y^2)} \delta_t^2 u_{i,j}^n = \Delta t^4 \left[c_{i,j} \frac{\partial^4 u}{\partial y^2 \partial t^2}\Big|_{i,j}^n \right] + O(h_y^6) + O(\Delta t^6). \tag{27}$$

Let $w(x, y, t) = c(x, y)\frac{\partial^4 u}{\partial y^2 \partial t^2}$, Eq. (22) can be written as

$$ERR = \Delta t^4 \, \frac{c_{i,j}}{144} \left[\frac{\Delta t^2}{h_x^2} \frac{\delta_x^2}{(1 + \frac{1}{12}\delta_x^2)} \, w_{i,j}^n \right] + O(h_y^6) + O(\Delta t^6)$$

$$= \Delta t^4 \, \frac{c_{i,j}}{144} \left[\frac{\Delta t^2}{h_x^2} \left(\delta_x^2 \left(1 - \frac{1}{12}\delta_x^2\right) w_{i,j}^n + O(h_x^6) \right) \right] + O(h_y^6) + O(\Delta t^6)$$

$$= \Delta t^4 \, \frac{c_{i,j}}{144} \left[\frac{\Delta t^2}{h_x^2} \left(\delta_x^2 \left(1 - \frac{1}{12}\delta_x^2\right) w_{i,j}^n + O(\Delta t^2 h_x^4) \right) \right] + O(h_y^6) + O(\Delta t^6)$$

$$= \Delta t^4 \, \frac{c_{i,j}}{144} \left[\frac{\Delta t^2}{h_x^2} \left(\delta_x^2 \left(1 - \frac{1}{12}\delta_x^2\right) w_{i,j}^n \right) \right] + O(\Delta t^6) + O(h_y^6). \tag{28}$$

Expanding $\delta_x^2 (1 - \frac{1}{12}\delta_x^2) w_{i,j}^n$ we obtain

$$\delta_x^2 \left(1 - \frac{1}{12}\delta_x^2\right) w_{i,j}^n = \frac{1}{12}\Big[-w_{i-2,j}^n + 16w_{i-1,j}^n - 30w_{i,j}^n + 16w_{i+1,j}^n - w_{i+2,j}^n\Big]. \tag{29}$$

Using Taylor series expansion, we can simplify it to

$$\delta_x^2 \left(1 - \frac{1}{12}\delta_x^2\right) w_{i,j}^n = h_x^2 \frac{\partial^2 w}{\partial x^2}\Big|_{i,j}^n - \frac{2h_x^6}{15} \frac{\partial^6 w(\xi_i, y_j, t_n)}{\partial x^6}, \tag{30}$$

where $\xi_i \in (x_{i-1}, x_{i+1})$.

Inserting Eq. (30) into Eq. (28) leads to

$$ERR = \Delta t^4 \, \frac{c_{i,j}}{144} \left[\Delta t^2 \frac{\partial^2 w}{\partial x^2}\Big|_{i,j}^n \right] + O(\Delta t^6) + O(h_y^6) = \Delta t^6 \, \frac{c_{i,j}}{144} \frac{\partial^2 w}{\partial x^2}\Big|_{i,j}^n + O(\Delta t^6) + O(h_y^6), \tag{31}$$

where

$$\frac{\partial^2 w}{\partial x^2} = \frac{\partial^2 c}{\partial x^2} \frac{\partial^4 u}{\partial y^2 \partial t^2} + 2 \frac{\partial c}{\partial x} \frac{\partial^5 u}{\partial x \partial y^2 \partial t^2} + c(x, y) \frac{\partial^6 u}{\partial x^2 \partial y^2 \partial t^2}. \tag{32}$$

Therefore, the factoring error is given by

$$ERR = \bar{M} \, \Delta t^6 + \tilde{M} \, h_y^6, \tag{33}$$

provided that the following functions and derivatives:

$$c(x, y), \quad \frac{\partial c(x, y)}{\partial x}, \quad \frac{\partial^2 c(x, y)}{\partial x^2}, \quad \frac{\partial^4 u(x, y, t)}{\partial y^2 \partial t^2}, \quad \frac{\partial^5 u(x, y, t)}{\partial x \partial y^2 \partial t^2}, \quad \frac{\partial^6 u(x, y, t)}{\partial x^2 \partial y^2 \partial t^2}$$

are bounded in $\Omega \times [0, T]$. $\bar{M}$ and $\tilde{M}$ are positive constants depending on the functions listed in Eq. (32). □

Remark. It is worthwhile to mention that one can factorize Eq. (20) using a different order of δ_x^2 and δ_y^2 and still get the same conclusion on the order of truncation error. For example, if Eq. (20) is factorized as

$$\left[1 - \frac{\lambda_y c_{i,j}}{12} \frac{\delta_y^2}{(1 + \frac{1}{12}\delta_y^2)}\right] \cdot \left[1 - \frac{\lambda_x c_{i,j}}{12} \frac{\delta_x^2}{(1 + \frac{1}{12}\delta_x^2)}\right] \delta_t^2 u_{i,j}^n = c_{i,j}\left[\lambda_x \frac{\delta_x^2}{(1 + \frac{1}{12}\delta_x^2)} + \lambda_y \frac{\delta_y^2}{(1 + \frac{1}{12}\delta_y^2)}\right] u_{i,j}^n$$
$$+ \Delta t^2 \left(1 + \frac{\delta_t^2}{12}\right) s_{i,j}^n + ERR, \qquad (34)$$

then the factoring error *ERR* is given by

$$ERR = \frac{\lambda_y}{144} c_{i,j} \frac{\delta_y^2}{(1 + \frac{1}{12}\delta_y^2)} \lambda_x c_{i,j} \frac{\delta_x^2}{(1 + \frac{1}{12}\delta_x^2)} \delta_t^2 u_{i,j}^n. \qquad (35)$$

Consequently, Eq. (32) will be modified to the following:

$$\frac{\partial^2 w}{\partial y^2} = \frac{\partial^2 c}{\partial y^2} \frac{\partial^4 u}{\partial x^2 \partial t^2} + 2\frac{\partial c}{\partial y} \frac{\partial^5 u}{\partial x^2 \partial y \partial t^2} + c(x,y)\frac{\partial^6 u}{\partial x^2 \partial y^2 \partial t^2}, \qquad (36)$$

where $w(x,y,t) = c(x,y)\frac{\partial^4 u(x,y,t)}{\partial x^2 \partial t^2}$. Under the same smoothness condition given in the theorem, we can derive the same error estimation as that given in Eq. (33).

Ignoring the factoring error leads to the following fourth-order compact FD method:

$$\left[1 - \frac{\lambda_x c_{i,j}}{12} \frac{\delta_x^2}{(1 + \frac{\delta_x^2}{12})}\right] \cdot \left[1 - \frac{\lambda_y c_{i,j}}{12} \frac{\delta_y^2}{(1 + \frac{\delta_y^2}{12})}\right] \delta_t^2 u_{i,j}^n = \left[\lambda_x c_{i,j} \frac{\delta_x^2}{(1 + \frac{\delta_x^2}{12})} + \lambda_y c_{i,j} \frac{\delta_y^2}{(1 + \frac{\delta_y^2}{12})}\right] u_{i,j}^n + \Delta t^2 \left(1 + \frac{\delta_t^2}{12}\right) s_{i,j}^n. \qquad (37)$$

Using ADI method, Eq. (37) can be efficiently solved in two steps

$$\left(1 - \frac{\lambda_x c_{i,j}}{12} \frac{\delta_x^2}{(1 + \frac{\delta_x^2}{12})}\right) u_{i,j}^* = \left[\lambda_x c_{i,j} \frac{\delta_x^2}{(1 + \frac{\delta_x^2}{12})} + \lambda_y c_{i,j} \frac{\delta_y^2}{(1 + \frac{\delta_y^2}{12})}\right] u_{i,j}^n + \Delta t^2 \left(1 + \frac{\delta_t^2}{12}\right) s_{i,j}^n, \qquad (38)$$

$$\left(1 - \frac{\lambda_y c_{i,j}}{12} \frac{\delta_y^2}{(1 + \frac{\delta_y^2}{12})}\right) \delta_t^2 u_{i,j}^n = u_{i,j}^*. \qquad (39)$$

However, both equations are difficult to implement due to the presence of $\left(1 + \frac{\delta_x^2}{12}\right)^{-1}$ and $\left(1 + \frac{\delta_y^2}{12}\right)^{-1}$. Divide $c_{i,j}$ then multiply $\left(1 + \frac{\delta_x^2}{12}\right)$ to both sides of Eq. (38), we have

$$\left[\left(1 + \frac{\delta_x^2}{12}\right)\frac{1}{c_{i,j}} - \frac{\lambda_x}{12}\delta_x^2\right] u_{i,j}^* = \left[\lambda_x \delta_x^2 + \lambda_y\left(1 + \frac{\delta_x^2}{12}\right)\frac{\delta_y^2}{(1 + \frac{\delta_y^2}{12})}\right] u_{i,j}^n + \Delta t^2 \left(1 + \frac{\delta_x^2}{12}\right)\left(1 + \frac{\delta_t^2}{12}\right)\frac{s_{i,j}^n}{c_{i,j}}. \qquad (40)$$

Eq. (40) is still not implementable because of the term $\frac{\delta_y^2}{(1 + \frac{\delta_y^2}{12})}$. Substituting $\frac{\delta_y^2}{1 + \frac{\delta_y^2}{12}} u_{i,j}^n$ with $\delta_y^2(1 - \frac{\delta_y^2}{12})u_{i,j}^n$, we obtain

$$\left[\left(1 + \frac{\delta_x^2}{12}\right)\frac{1}{c_{i,j}} - \frac{\lambda_x}{12}\delta_x^2\right] u_{i,j}^* = \left[\lambda_x \delta_x^2 + \lambda_y\left(1 + \frac{\delta_x^2}{12}\right)\delta_y^2\left(1 - \frac{\delta_y^2}{12}\right)\right] u_{i,j}^n + \Delta t^2 \left(1 + \frac{\delta_x^2}{12}\right)\left(1 + \frac{\delta_t^2}{12}\right)\frac{s_{i,j}^n}{c_{i,j}},$$
$$j = 2, 3, \cdots, N_y - 1. \qquad (41)$$

Notice the difference between Eqs. (40) and (41) is $O(h_y^6)$, thus, the method is still fourth-order accurate in space.

Similarly, divide $c_{i,j}$ then multiply $\left(1 + \frac{\delta_y^2}{12}\right)$ to both sides of Eq. (39), we have

$$\left[\left(1 + \frac{\delta_y^2}{12}\right)\frac{1}{c_{i,j}} - \frac{\lambda_y}{12}\delta_y^2\right] \delta_t^2 u_{i,j}^n = \left(1 + \frac{\delta_y^2}{12}\right)\frac{u_{i,j}^*}{c_{i,j}}, \quad i = 2, 3, \ldots, N_x - 1. \qquad (42)$$

Eq. (42) is equivalent to the following three-level FD scheme:

$$\left[\left(1 + \frac{\delta_y^2}{12}\right)\frac{1}{c_{i,j}} - \frac{\lambda_y}{12}\delta_y^2\right] u_{i,j}^{n+1} = \left[\left(1 + \frac{\delta_y^2}{12}\right)\frac{1}{c_{i,j}} - \frac{\lambda_y}{12}\delta_y^2\right](2u_{i,j}^n - u_{i,j}^{n-1}) + \left(1 + \frac{\delta_y^2}{12}\right)\frac{u_{i,j}^*}{c_{i,j}}, \quad i = 2, 3, \ldots, N_x - 1. \qquad (43)$$

Both Eqs. (41) and (43) can be efficiently solved as sequence of decoupled tri-diagonal linear systems using Thomas algorithm. Here we point out that in Eq. (43), the following fourth-order one-sided approximations will be used to approximate $u_{i,1}^*$ and u_{i,N_y}^*, respectively.

$$u_{i,1}^* = 4u_{i,2}^* - 6u_{i,3}^* + 4u_{i,4}^* - u_{i,5}^*, \; i = 2, 3, \ldots, N_x - 1, \tag{44}$$

$$u_{i,N_y}^* = 4u_{i,N_y-1}^* - 6u_{i,N_y-2}^* + 4u_{i,N_y-3}^* - u_{i,N_y-4}^*, \; i = 2, 3, \ldots, N_x - 1. \tag{45}$$

The boundary conditions needed for Eq. (41) can be obtained by setting $i = 1$ and $i = N_x$ in Eq. (42), respectively.

$$\left(1 + \frac{\delta_y^2}{12}\right)u_{1,j}^* = \left[\left(1 + \frac{\delta_y^2}{12}\right)\frac{1}{c_{i,j}} - \frac{\lambda_y}{12}\delta_y^2\right]\delta_t^2 u_{1,j}^n, \tag{46}$$

$$\left(1 + \frac{\delta_y^2}{12}\right)u_{N_x,j}^* = \left[\left(1 + \frac{\delta_y^2}{12}\right)\frac{1}{c_{i,j}} - \frac{\lambda_y}{12}\delta_y^2\right]\delta_t^2 u_{N_x,j}^n. \tag{47}$$

Solving the two tri-diagonal linear systems, we can get the boundary conditions for Eq. (41).

The new compact fourth-order ADI method is a three-level FD scheme, which requires two initial conditions. However, only the first initial condition is explicitly specified. To approximate the second initial condition with higher-order (fourth-order in this case) accuracy, we develop the following approach. Expanding $u(x_i, y_j, \Delta t)$ by Taylor series at $t = 0$ we obtain the following fourth-order approximation:

$$
\begin{aligned}
u(x_i, y_j, \Delta t) &= u_{i,j}^0 + \Delta t u_t(x_i, y_j, 0) + \frac{\Delta t^2}{2}u_{tt}(x_i, y_j, 0) + \frac{\Delta t^3}{6}u_{ttt}(x_i, y_j, 0) + \frac{\Delta t^4}{24}u_{tttt}(x_i, y_j, 0) + O(\Delta t^5) \\
&= u_{i,j}^0 + \Delta t f_2(x_i, y_j) + \frac{\Delta t^2}{2}(c_{i,j}\triangle f_1(x_i, y_j) + s(x_i, y_j, 0)) + \frac{\Delta t^3}{6}(c_{i,j}\triangle f_2(x_i, y_j, 0) + s_t(x_i, y_j, 0)) \\
&\quad + \frac{\Delta t^4}{24}[\{c(x,y)\triangle(c(x,y)\triangle f_1 + s(x,y,0))\}|_{i,j} + s_{tt}(x_i, y_j, 0)] + O(\Delta t^5),
\end{aligned}
\tag{48}
$$

where $\triangle$ represents the Laplacian operator.

Now we state and prove the main result on the convergence of the compact ADI FD scheme defined in Eq. (37).

Theorem 3.2. *Assume that* $u(x, y, t) \in C_{x,y,t}^{6,6,6}(\Omega \times [0, T])$ *is the solution of the acoustic wave Eqs. (1)–(4), and the coefficient function satisfies the smooth condition* $c(x, y) \in C_x^2(\Omega)$. *Then the compact ADI FD scheme defined in Eq. (37) is fourth-order accurate in time and space with the truncation error* $O(\Delta t^4 + h_x^4 + h_y^4)$.

Proof. According to Theorem 3.1, if $u(x, y, t)$ and $c(x, y)$ are sufficiently smooth as required, the difference between the numerical scheme defined in Eq. (37) and the numerical scheme defined in Eq. (20) is $O(\Delta t^6) + O(h_y^6)$.

On the other hand, it is known [6] that the compact Padé approximation FD method defined in Eq. (37) is fourth-order in time and space, with the truncation error $O(\Delta t^4) + O(h_x^4) + O(h_y^4)$.

Moreover, one can see that the truncation errors caused by the substitution

$$\frac{\delta_y^2}{(1 + \frac{\delta_y^2}{12})} \to \delta_y^2\left(1 - \frac{\delta_y^2}{12}\right)$$

in Eq. (41) is $O(h_y^6)$.

Based on these, the new compact ADI FD scheme is fourth-order in time and space. □

4. Stability analysis

It is well known that most of the FD schemes for solving the acoustic wave equation are conditionally stable and subject to constraints on time step. Here we analyze the stability of the new method using the Von Neumann stability analysis. It is worthy to mention that the Von Neumann stability analysis is applicable to the constant velocity case only. Although it is difficult to apply the von Neumann analysis method to the heterogeneous case directly, it is reported that one can replace $c(x, y)$ with c_{max}, which is the maximal value of $c(x, y)$ in Ω, then work on the acoustic wave equation with constant velocity c_{max}. In this section, we conduct the stability analysis using c_{max} as the constant velocity. The conclusion on the CFL condition will be numerically verified later. For the sake of simplicity, we assume that $h_x = h_y = h$ and $s(x, y, t) \equiv 0$. Such simplification does not affect the conclusion in general. The main result on the stability is stated in the following theorem:

Theorem 4.1. *Assume that the solution of the acoustic wave equation Eq. (1) is sufficiently smooth, the compact fourth-order ADI FD scheme defined in Eq. (37) is stable if*

$$\frac{\sqrt{c_{max}}\,\Delta t}{h} < \sqrt{4 - 2\sqrt{3}} \approx 0.7321, \tag{49}$$

where

$$c_{max} = \max_{(x,y)\in\Omega} c(x,y).$$

Proof. Let $\nu = \sqrt{c_{max}}$, $r = \frac{\nu^2 \Delta t^2}{h^2}$, $\rho = \frac{1-r}{12}$, the numerical scheme is given by

$$\frac{\delta_t^2}{(1 + \frac{\delta_t^2}{12})} u_{i,j}^n = r\left(\frac{\delta_x^2}{(1 + \frac{\delta_x^2}{12})} + \frac{\delta_y^2}{(1 + \frac{\delta_y^2}{12})}\right) u_{i,j}^n,$$

which is equivalent to

$$\left[\left(1 + \frac{\delta_x^2}{12}\right)\left(1 + \frac{\delta_y^2}{12}\right) - \frac{r}{12}\left(\left(1 + \frac{\delta_x^2}{12}\right)\delta_y^2 + \left(1 + \frac{\delta_y^2}{12}\right)\delta_x^2\right)\right]\delta_t^2 u_{i,j}^n = r\left[\left(1 + \frac{\delta_x^2}{12}\right)\delta_y^2 + \left(1 + \frac{\delta_y^2}{12}\right)\delta_x^2\right]u_{i,j}^n. \tag{50}$$

After simplifying it, we have

$$[(1 + \rho\delta_x^2)(1 + \rho\delta_y^2)]u_{i,j}^{n+1} - \left[2(1 + \rho\delta_x^2)(1 + \rho\delta_y^2) + r\left(1 + \frac{1}{12}\delta_x^2\right)\delta_y^2 + r\left(1 + \frac{1}{12}\delta_y^2\right)\delta_x^2\right]u_{i,j}^n$$

$$+ [(1 + \rho\delta_x^2)(1 + \rho\delta_y^2)]u_{i,j}^{n-1} = 0. \tag{51}$$

Taking discrete Fourier transformation of Eq. (51) yields

$$\left(1 - 4\rho \sin^2\left(\frac{\theta}{2}\right)\right)\left(1 - 4\rho \sin^2\left(\frac{\xi}{2}\right)\right)\hat{u}^{n+1} - \left[2\left(1 - 4\rho \sin^2\left(\frac{\theta}{2}\right)\right)\left(1 - 4\rho \sin^2\left(\frac{\xi}{2}\right)\right)\right.$$

$$\left. - 4r\sin^2\left(\frac{\theta}{2}\right)\left(1 - \frac{1}{3}\sin^2\left(\frac{\xi}{2}\right)\right) - 4r\sin^2\left(\frac{\xi}{2}\right)\left(1 - \frac{1}{3}\sin^2\left(\frac{\theta}{2}\right)\right)\right]\hat{u}^n$$

$$+ \left(1 - 4\rho \sin^2\left(\frac{\theta}{2}\right)\right)\left(1 - 4\rho \sin^2\left(\frac{\xi}{2}\right)\right)\hat{u}^{n-1} = 0, \tag{52}$$

where $\hat{u}^n$ represents the discrete Fourier transform of $u_{i,j}^n$ at time level t_n.

Since $\rho = \frac{1-r^2}{12}$, $1 - 4\rho \sin^2\left(\frac{\theta}{2}\right) = 1 - \frac{1}{3}\sin^2\left(\frac{\theta}{2}\right) + \frac{r^2}{3}\sin^2\left(\frac{\theta}{2}\right) > 0$. Similarly, we can show that $1 - 4\rho \sin^2\left(\frac{\xi}{2}\right) > 0$ as well.

Let $s_\theta = \sin\left(\frac{\theta}{2}\right)$, $s_\xi = \sin\left(\frac{\xi}{2}\right)$, Eq. (52) is simplified as

$$\hat{u}^{n+1} + \varrho(\theta, \xi)\hat{u}^n + \hat{u}^{n-1} = 0, \tag{53}$$

where

$$\varrho(\theta, \xi) = -2 + \frac{r}{3}\left[\frac{12(s_\theta^2 + s_\xi^2) - 8s_\theta^2 s_\xi^2}{(1 - -4\rho s_\theta^2)(1 - -4\rho s_\xi^2)}\right]. \tag{54}$$

The characteristic equation of Eq. (53) is given by

$$P(z) = z^2 + \varrho(\theta, \xi)z + 1 = 0. \tag{55}$$

To ensure that the fourth-order compact FD scheme in Eq. (53) is stable, we need

$$|\varrho(\theta, \xi))| < 2 \iff -2 < \varrho(\theta, \xi)) < 2, \tag{56}$$

which is the sufficient condition for stability.

Since $s_\theta^2 \le 1$, $s_\xi^2 \le 1$, we have

$$12(s_\theta^2 + s_\xi^2) - 8s_\theta^2 s_\xi^2 = 8s_\theta^2(1 - s_\xi^2) + 4s_\theta^2 + 12s_\xi^2 \ge 0, \tag{57}$$

which indicates that $\varrho(\theta, \xi) > -2$.

We now show that $\varrho(\theta, \xi) < 2$ is true under the stability condition given in the theorem. First, we observe that

$$\varrho(\theta, \xi) < 2 \Leftrightarrow \frac{r}{3}\left[\frac{12(s_\theta^2 + s_\xi^2) - 8s_\theta^2 s_\xi^2}{(1 - -4\rho s_\theta^2)(1 - -4\rho s_\xi^2)}\right] < 4. \tag{58}$$

Using the definition $\rho = \frac{1-r}{12}$, we define

$$\chi(s_\theta^2, s_\xi^2) = \frac{12(s_\theta^2 + s_\xi^2) - 8s_\theta^2 s_\xi^2}{\left[\left(1 - \frac{s_\theta^2}{3}\right) + \frac{r}{3}s_\theta^2\right]\left[\left(1 - \frac{s_\xi^2}{3}\right) + \frac{r}{3}s_\xi^2\right]}.$$

Table 1
Maximal errors for **example 1** with $\Delta t = 0.001$ at $T = 1$.

h	$\pi/40$	$\pi/80$	$\pi/160$	$\pi/320$
CPU time(s)	6.4300	22.589	100.77	1703.8
$E_M(h)$	5.8198e−07	2.8575e−08	1.4868e−09	7.0404e−11
$\frac{E_M(h)}{E_M(h/2)}$	–	20.367	19.219	21.119
Conver. order	–	4.3481	4.2645	4.4004

Table 2
Maximal errors for **example 1** with various h and Δt.

$(h, \Delta t)$	$(\pi/40, 1/80)$	$(\pi/80, 1/160)$	$(\pi/160, 1/320)$	$(\pi/320, 1/640)$
CPU time(s)	0.59	3.34	28.56	221.09
$E_M(h, \Delta t)$	5.3696e−07	2.325e−08	8.4585e−10	3.2258e−11
$\frac{E_M(h, \Delta t)}{E_M(h/2, \Delta t/2)}$	–	23.0918	27.4911	26.2215
Conver. order	–	4.5293	4.7809	4.7127

Table 3
Maximal errors for **example 2** with various h and Δt.

$(h, \Delta t)$	$(\pi/40, 1/80)$	$(\pi/80, 1/160)$	$(\pi/160, 1/320)$	$(\pi/320, 1/640)$
$E_M(h, \Delta t)$	2.7242e−06	2.2523e−07	1.7543e−08	1.2928e−09
$\frac{E_M(h, \Delta t)}{E_M(h/2, \Delta t/2)}$	–	12.09519	12.8387	13.5697
Conver. order	–	3.59636	3.682427	3.762317

If $r = 1$, then $\chi(1, 1) = 16$, the inequality in Eq. (58) is not satisfied, hence the method is not stable. Therefore, we consider $r < 1$ only. Apparently, when $r < 1$, the numerator of χ is an increasing function of s_θ^2 and s_ξ^2, while the denominator of χ is a decreasing function of s_θ^2 and s_ξ^2. Consequently χ reaches its maximum when $(s_\theta^2, s_\xi^2) = (1, 1)$.

From Eq. (58), we have

$$r \cdot \chi(1, 1) < 12 \Rightarrow \frac{16r}{(\frac{2}{3} + \frac{r}{3})^2} < 12.$$

Given that $0 < r < 1$, we obtain the following CFL condition:

$$r < 4 - \sqrt{3} \Rightarrow \frac{\sqrt{c_{max}}\,\Delta t}{h} < \sqrt{4 - \sqrt{3}} \approx 0.7321.$$

Finally, the compact fourth-order ADI method defined in Eq. (37) is stable if

$$\frac{\sqrt{c_{max}}\,\Delta t}{h} < \sqrt{4 - \sqrt{3}}. \qquad \square$$

5. Numerical examples

In this section five numerical examples are solved by the new method to demonstrate the efficiency and accuracy. The first and the second examples, whose exact solutions are available, are used to validate the order of convergence of the numerical method.

5.1. Example 1

We first solve the acoustic wave equation given in Eq. (1) on a rectangular domain $[0, \pi] \times [0, \pi]$ with $t \in [0, 1]$, for which the analytical solution is available as $u(x, y, t) = \cos(t)\sin(x)\sin(y)$. The initial and boundary conditions are chosen accordingly to satisfy the analytical solution. The spatially varying velocity model is chosen as $c(x, y) = 1 + \left(\frac{x}{\pi}\right)^2 + \left(\frac{y}{\pi}\right)^2$ to accommodate the exact solution and the source function, which is given by

$$s(x, y, t) = \left(1 + 2\left(\frac{x}{\pi}\right)^2 + 2\left(\frac{y}{\pi}\right)^2\right)\cos(t)\sin(x)\sin(y).$$

It is noted that this problem has zero boundary condition, which is chosen to simplify programming. A more general example with non-zero boundary condition will be solved in the next example. To simplify the discussion, uniform grid size h is used in x and y directions. To validate the fourth-order convergence in space, we fixed $\Delta t = 0.001$ so the temporal truncation error is negligible. The maximal errors are included in Table 1, which clearly show that the new method is fourth-order accurate in space, as the errors are reduced roughly by a factor 16 when h is reduced by a factor 2. We notice

Table 4
Maximal errors for **example 2** with $h = \pi/200$ and various Δt.

Δt	1/147	1/148	1/149	1/150	1/151
Δt in decimal	0.00680	0.00676	0.00671	0.00667	0.00662
$E_M(h, \Delta t)$	0.03347	1.2298e−07	8.1505e−09	8.1398e−09	8.1293e−09

Table 5
Comparison of maximum errors for various methods with $\frac{\Delta t}{h} = 0.5$.

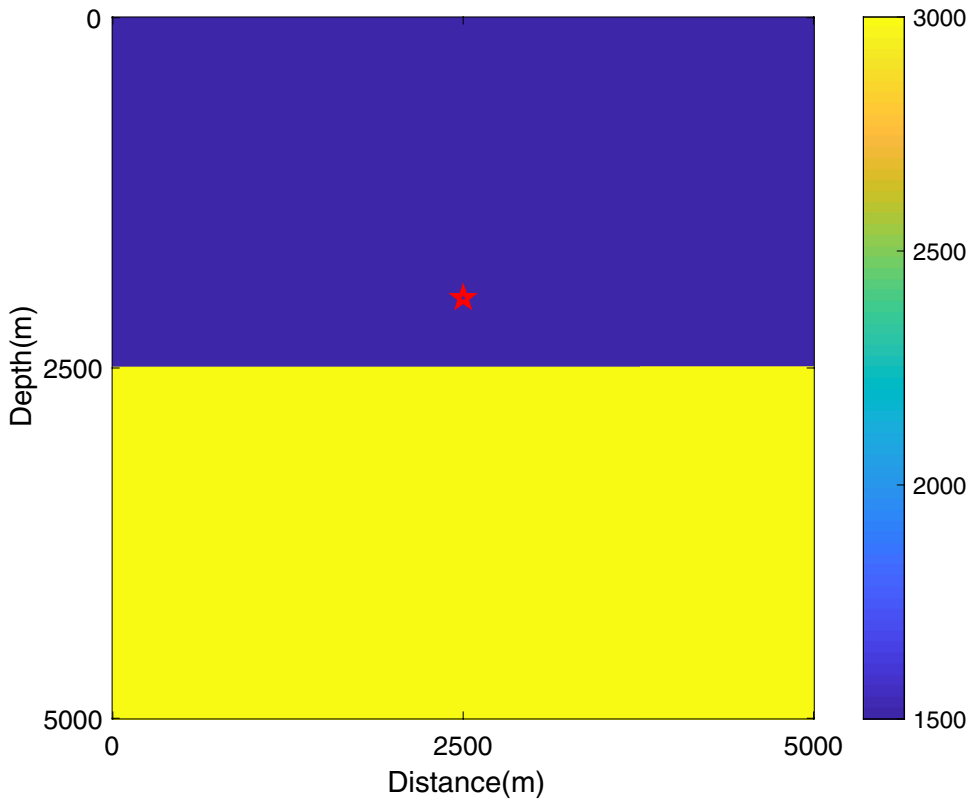| $(h, \Delta t)$	NCV-CPD-ADI	HOC-LOD	CPD-ADI	IPD-ADI
(1/5, 1/10)	1.5476e−06	9.6829e−07	1.2670e−06	1.2670e−06
(1/10, 1/20)	1.0897e−07	4.2143e−08	7.6259e−08	1.8736e−08
(1/20, 1/40)	6.9950e−09	2.4180e−09	4.7401e−09	2.3039e−09
(1/40, 1/80)	4.6076e−10	1.5111e−10	2.9388e−10	1.5999e−10
(1/80, 1/160)	3.0854e−11	1.2392e−11	1.8150e−11	1.0401e−11

Fig. 1. Velocity model consisting of two homogeneous layers with constant acoustic velocity 1500 m/s in the upper layer, and constant velocity 3000 m/s in the lower layer. The red star indicates source which is located at (2500 m, 2000 m). (For interpretation of the references to color in this figure legend, the reader is referred to the web version of this article.)

that the convergence order is slightly higher than fourth-order. One possible reason is that the numerical error is randomly canceled during the computation process.

To show that the method is fourth-order accurate in time, h and Δt are simultaneously reduced by a factor of 2 to ensure that the CFL condition is satisfied. We mention that using very small fixed h to verify the order in time will violate the stability condition. Instead we verify the order of convergence in time through the following contradiction argument. Suppose the numerical scheme is pth-order accurate in time and fourth-order in space, with $p < 4$, halving h and Δt several times, the truncation error in time will become the dominating error, thus, the total error will be reduced by a factor of $2^p < 16$ when h and Δt been halved. In the following numerical test cases, we start from $h = \pi/40$, $\Delta t = 1/80$ (the parameters are chosen to satisfy the stability condition) and each time we halve both h and Δt. The result in Table 2 clearly indicates that the total error is reduced by a factor 16 (roughly) when h and Δt are halved, which confirmed that the convergence order in time is four.
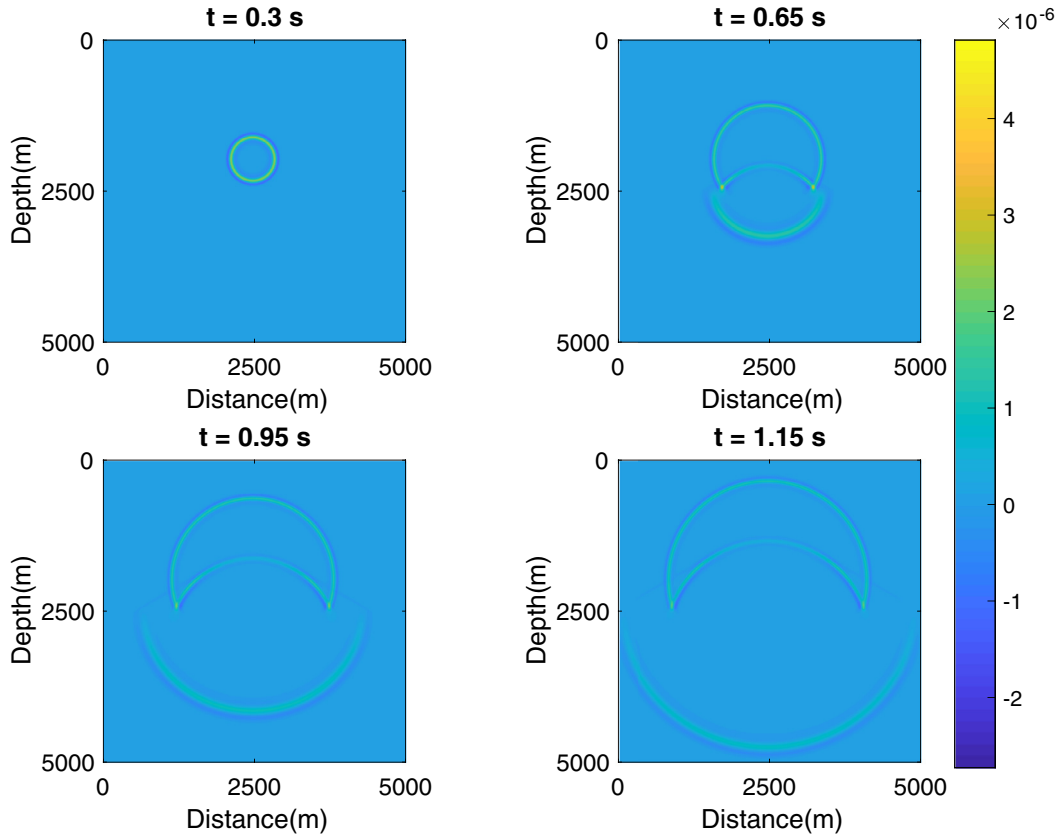
Fig. 2. Wavefields snapshots computed by the fourth-order compact ADI algorithm for the two-layer model: (a) $t = 0.3$ s; (b) $t = 0.65$ s; (c) $t = 0.95$ s; (d) $t = 1.15$ s.

Furthermore, it is clear that the new method has linear complexity with problem size. In Table 1, when Δt is fixed, if h is halved, the total number of grid points is increased by a factor 4, consequently the CPU time is increased by a factor 4. While in Table 2, when both Δt and h are halved, the total number of grid point is increased by a factor 4, and the number of time steps is doubled, so the problem size is increased by a factor of 8. Consequently the CPU time is increased by a factor 8.

It is worthy to point out that, the new method is an implicit scheme, therefore, the computational cost in each time step is higher than that of the explicit method. However, the overall computational efficiency has been greatly improved due to the higher-order of convergence.

5.2. Example 2

In this example we solve an acoustic wave equation with non-zero boundary condition. The coefficient is chosen as $c(x, y) = 1 + \sin^2(x) + \sin^2(y)$. The exact solution is available as $u(x, y, t) = e^{-t} \cos(x) \cos(y)$. The initial conditions and source function are chosen accordingly to satisfy the exact solution and the equation.

The purpose of this example is two-fold. First, we use this example to further confirm that the new method is fourth-order in time and space for a wave equation with non-zero boundary conditions. To this end, the acoustic wave equation is solved with various h and Δt, and the numerical result is listed in Table 3. It is clear that when h and Δt are halved, the maximal error is reduced roughly by a factor of 16, which indicates fourth-order convergence in both time and space.

Secondly, we use this example to verify the stability condition of the new method derived in Theorem 4.1. Due to the heterogeneity of the media, it is difficult, if not impossible to apply Von Neumann stability analysis, which is applicable to homogeneous case only. However it is well-known that the CFL condition is determined by the maximal value of $c(x, y)$ in the domain Ω. Thus, the conjecture is that the stability condition or the constraint is given by

$$\sqrt{c_{max}} \, \frac{\Delta t}{h} < \sqrt{4 - 2\sqrt{3}},$$

where

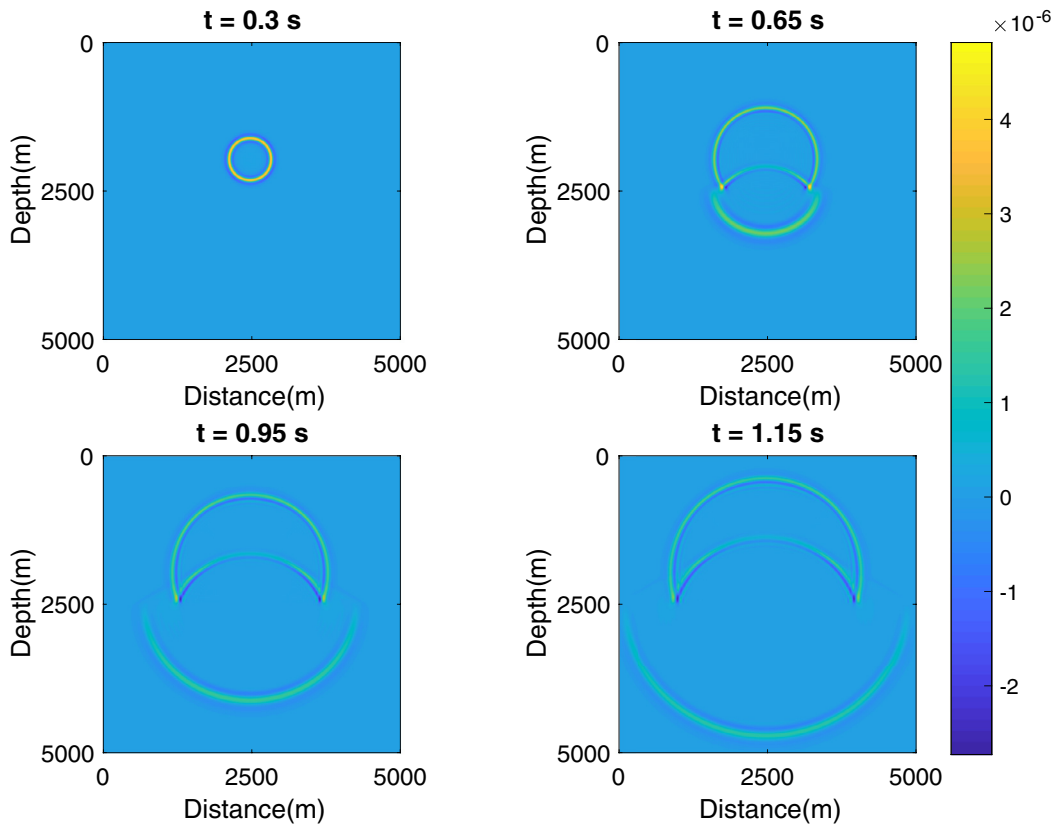$$c_{max} = \max_{(x,y) \in [0,\pi] \times [0,\pi]} 1 + \sin^2(x) + \sin^2(y) = 3.$$

Fig. 3. Wavefields snapshots computed by the standard second-order finite difference algorithm for the two-layer model: (a) $t = 0.3$ s; (b) $t = 0.65$ s; (c) $t = 0.95$ s; (d) $t = 1.15$ s.

Therefore, the CFL condition is

$$\frac{\Delta t}{h} < \frac{0.7321}{\sqrt{3}} \approx 0.4226.$$

To verify this conjecture, we fix $h = \pi/200$. By the conjecture, the CFL condition is given by

$$\Delta t < 0.4226 * \pi/200 \approx 0.006638185. \tag{59}$$

Simple calculation shows that $\frac{1}{150} < 0.006638185 < \frac{1}{151}$. We run the code with several Δt near 1/150. The result is listed in Table 4, which shows that error is consistent when $\Delta t \leq 1/149$. However, the error increases significantly when Δt increases to 1/148. When Δt gets larger, the error increases even faster, and eventually blows out due to violation of the stability condition. Note that the CFL condition given in Eq. (59) is a sufficient condition. Base on the experiment, one can see that the theoretical stability condition given in Theorem 4.1 is very accurate.

5.3. Example 3

In this example we solve the problem with a point source located inside a $[0, 5\,\text{km}] \times [0, 5\,\text{km}]$ two-layer model, as shown in Fig. 1. The upper half is a homogenous layer with $v = 1500\,\text{m/s}$, while the lower half is a homogeneous layer with $v = 3000\,\text{m/s}$. The Ricker's wavelet source that generates the wave is given by

$$s(x, y, t) = \delta(x - x_0, y - y_0)\left[1 - 2\pi^2 f_p^2 (t - d_r)^2\right] e^{-\pi^2 f_p^2 (t - d_r)^2},$$

where $f_p = 10\,\text{Hz}$ is the peak frequency. Here, $d_r = 0.5/f_p$ is the temporal delay that is used to ensure zero initial conditions and $\delta(x - x_0, y - y_0)$ is the Dirac delta distribution. For all numerical simulations, the uniform grid size $h = h_x = h_y = 12.5\,\text{m}$ is used, $\Delta t = 0.001$ s is chosen accordingly such that the CFL condition defined in Eq. (49) is satisfied.

To simplify the boundary condition treatment, zero boundary conditions will be implemented. However, we point out that such treatment is inappropriate in realistic situation, in which one should consider implementing absorbing boundary condition or perfectly matched layered condition, which apparently beyond the scope of this work.

We plot the snapshots of wavefields at various simulation times. Because of the temporal delay, the wave source is ignited roughly at $t = 0.05$ s. Therefore, at $t = 0.3$ s, the wave propagates inside the upper layer only. Since the velocity is a
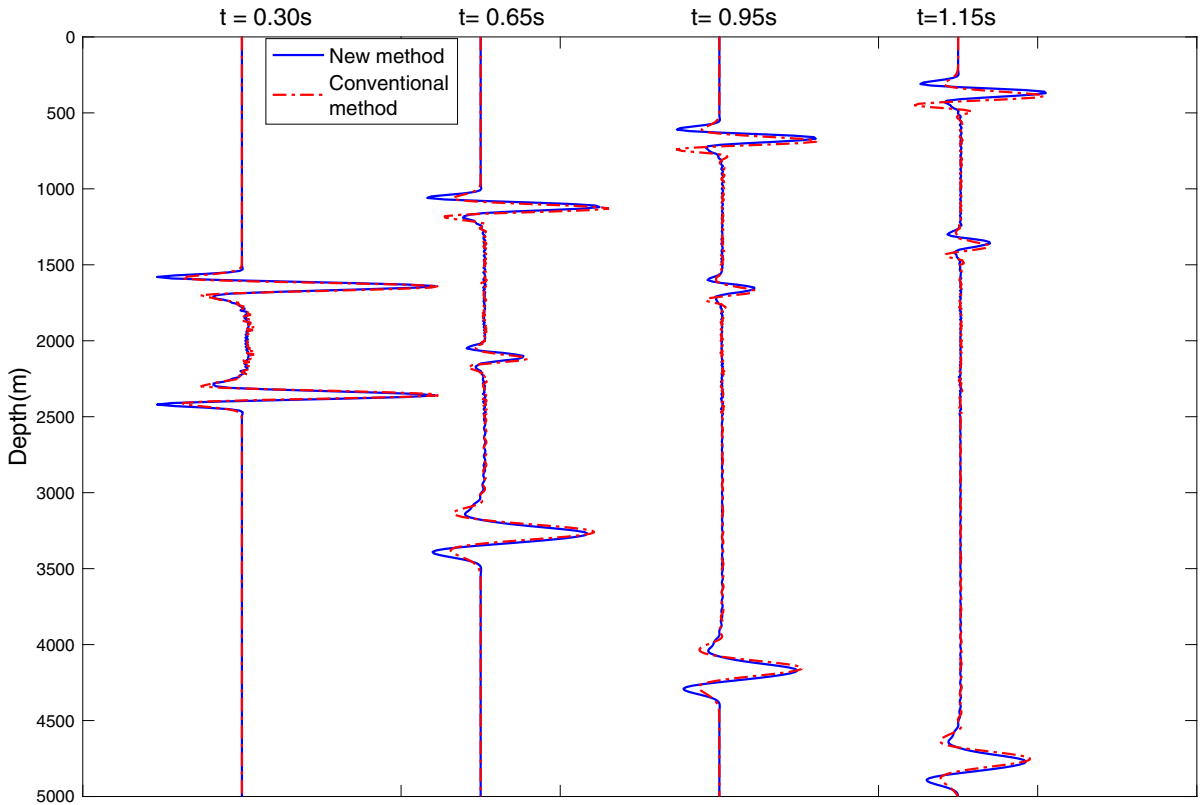
Fig. 4. Comparison of the amplitudes of wavefields computed by the new method (fourth-order compact ADI algorithm) and the conventional second-order central finite difference method. The wavefields are sampled at $x = 2500$ m for $t = 0.3$ s, 0.65 s, 0.95 s and 1.15 s. (For interpretation of the references to color in this figure legend, the reader is referred to the web version of this article.)

constant inside the upper half, the wavefront forms a perfect circle, as shown in Fig. 2(a). It is obvious that the wave front forms a perfect circle before it hits the interface of two layers, which confirms the accuracy of the numerical results. With simulation time increases, reflection can be observed near the interface. For example, as shown in Fig. 2(b), when $t = 0.65$ s, the wave front hits the interface and some moderate reflection can be observed. Since the velocities in both layers are constants, the reflected wavefront and refracted wavefront form perfect circles with different radius, in the upper half and the lower half of the domain, respectively. Similarly, in Fig. 2(c), when $t = 0.95$ s, both the reflected and refracted waves propagate further and form perfect circle wavefronts. Finally, in Fig. 2(d), the wavefront slightly hits the left and right sides of the domain and induces reflections. It is observed that there is nearly no visible artifact numerical dispersion in the four wavefield snapshots, which indicates that the new method is very effective in suppressing numerical dispersion.

For comparison, we implemented the standard second-order FD scheme. The wavefield snapshots are shown in Fig. 3. Clearly the second-order method is less accurate and produces visible numerical dispersion. In particular the curve of $t = 0.65$ s clearly shows the difference.

To demonstrate that the higher-order compact ADI method is more effective than the standard second-order FD method in suppressing numerical dispersion, the wavefields computed by the new fourth-order compact algorithm (blue solid line) and the conventional second-order method (red dashed line) at $x = 2500$ m are plotted in Fig. 4. Although both methods can produce reasonably accurate results, one can easily see that the new method is less dispersive. To further demonstrate the effectiveness of the new method in numerical dispersion reduction, the amplitudes of wavefields for $t = 0.3$ s and $t = 0.65$ are zoomed in and included in Fig. 5, which clearly shows that the new method is less dispersive.

Remark. Although the layered velocity model is not differentiable in y direction, the higher-order compact ADI method is still very accurate. This can be explained by the fact that $c(x, y)$, $\frac{\partial c}{\partial x}$ and $\frac{\partial^2 c}{\partial x^2}$ in Eq. (32) are continuous and bounded. As a matter of fact, $\frac{\partial c}{\partial x} = 0$, $\frac{\partial^2 c}{\partial x^2} = 0$.

5.4. Example 4

In this example we test the fourth-order compact ADI algorithm on the challenging Marmousi model, which is shown in Fig. 6. The same Ricker's wavelet source is used, with a slightly different time delay $d_r = 0.3/f_p$. The velocity model is
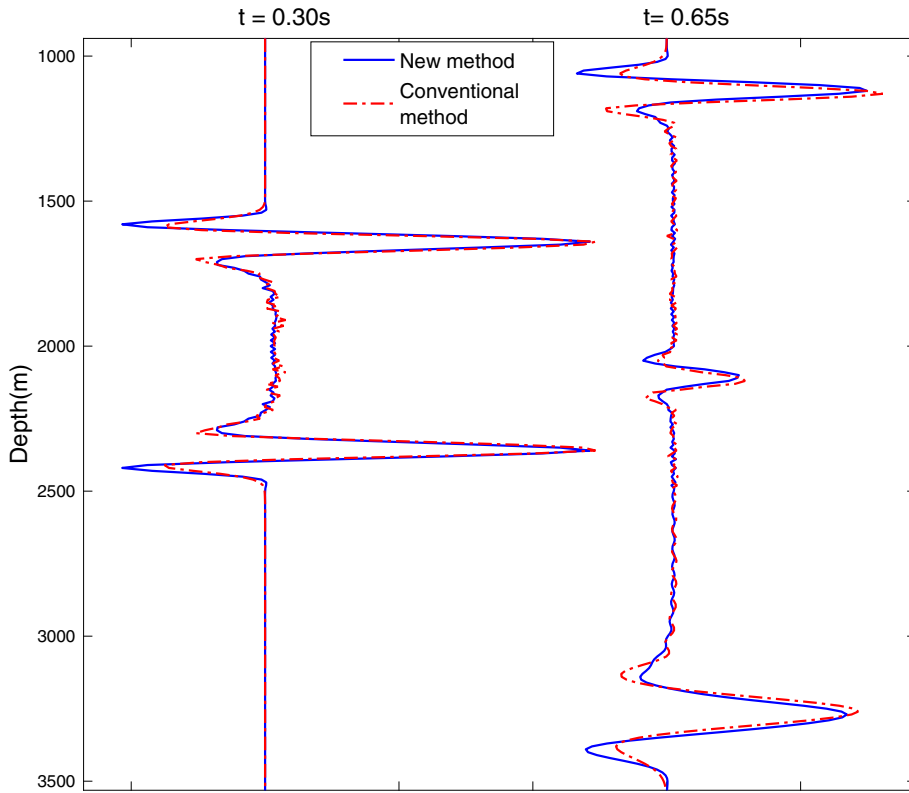
Fig. 5. Magnified amplitudes of wavefields at $x = 2500\,\mathrm{m}$ for $t = 0.3\,\mathrm{s}$ and $t = 0.65\,\mathrm{s}$.
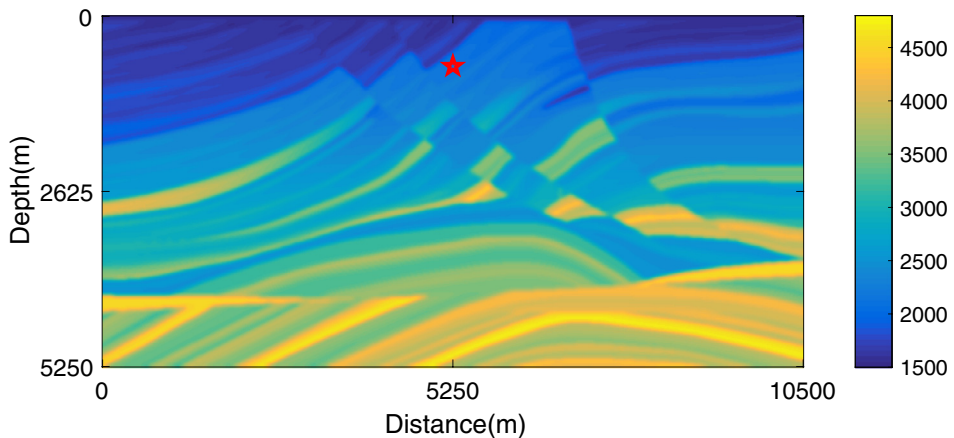

Fig. 6. Marmousi model defined on a $10500\,\mathrm{m} \times 5250\,\mathrm{m}$ rectangular domain. The velocity ranges from 1500 m/s to 4800 m/s. The source, denoted by the red star, is located at $(5250\,\mathrm{m}, 750\,\mathrm{m})$. (For interpretation of the references to color in this figure legend, the reader is referred to the web version of this article.)

defined on a 701×351 grid with uniform spacing $h = 15\,\mathrm{m}$, which defines a $[0, 10500\,\mathrm{m}] \times [0, 5250\,\mathrm{m}]$ rectangular domain. The computed waveform shown in Fig. 7 matches the velocity model very well. For example, visible reflections can be observed at points where velocity varies drastically. At the same time, only minor dispersion can be observed near the points with drastical velocity change. For comparison, the wavefields computed by the conventional second-order finite difference method at various times (*left column*) are shown side by side with the wavefields computed by the new method (*right column*) in Fig. 7. It is clear that the new method is more effective in suppressing numerical dispersion.
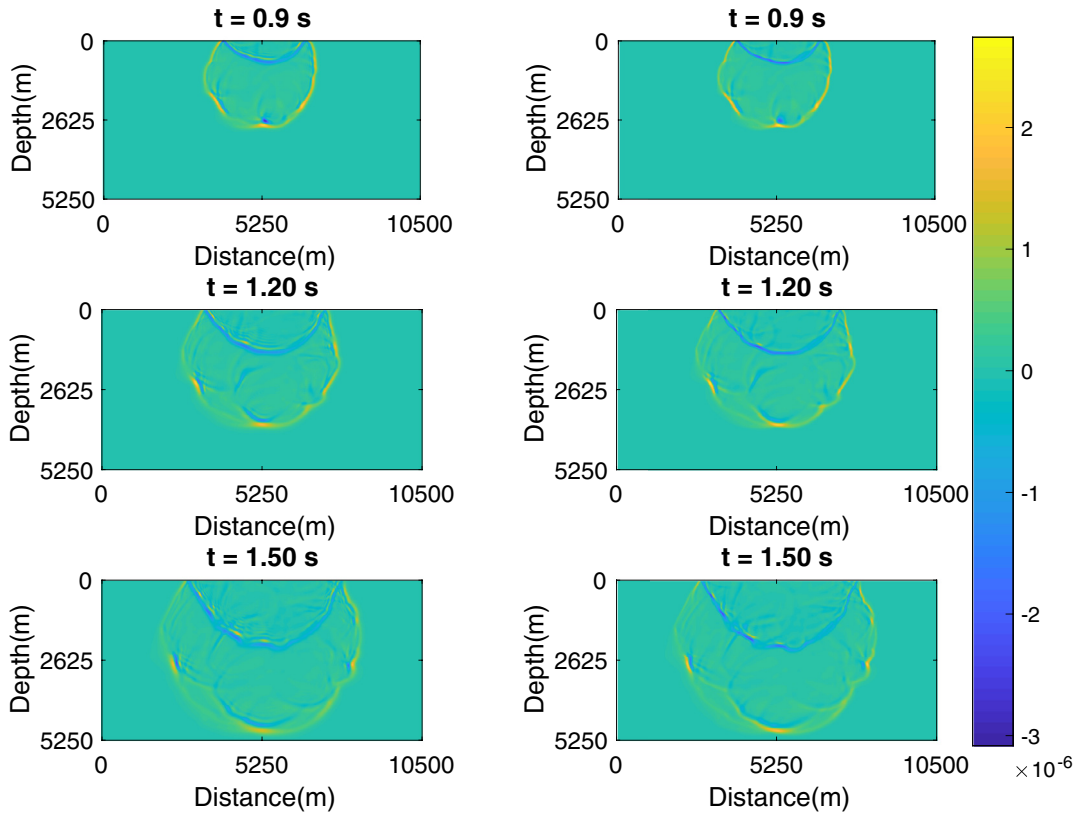
Fig. 7. Comparision of wavefields with Marmousi model computed by the conventional second-order FD method and the fourth-order compact ADI metod at $t = 0.9,\ 1.2,\ 1.5$ s. *Left column* - Wavefields computed by the conventional second-order FD scheme; *Right column* - Wavefields computed by the new fourth-order compact ADI method.

5.5. Example 5

Finally, we compare the new algorithm with other fourth-order methods proposed in [6,32] in terms of accuracy. We compare the new method with HOC-LOD that was proposed in [32] and two other methods: CPD-ADI and IPD-ADI that were proposed in [6]. The new method is denoted as NCV-CPD-ADI, which means non-constant velocity compact ADI method. The constant velocity problem to be solved is defined as

$$\frac{1}{v^2}\frac{\partial^2 u}{\partial t^2} = \frac{\partial^2 u}{\partial x^2} + \frac{\partial^2 u}{\partial y^2}, \quad (x, y, t) \in [0, 1] \times [0, 1] \times [0, T], \tag{60}$$

where $v = 1$ is the wave propagation velocity. The initial conditions are

$$u(x, y, 0) = \cos(-x - y), \quad \frac{\partial u(x, y, 0)}{\partial t} = -\sqrt{2}\sin(-x - y),$$

while the boundary conditions are chosen accordingly so that the analytical solution is

$$u(x, y, t) = \cos\big(\sqrt{2}t - x - y\big).$$

We solve this initial-boundary value problem for $T = 1$, and compute the maximum norm errors by various methods to compare the accuracy. For simplicity, we take $h_x = h_y$ in all numerical test cases. The numerical results are included in Table 5.

First, the fourth-order accuracy in space and time is clearly demonstrated for all methods, as can be seen in Table 5. The numerical data also shows that the new algorithm is the least accurate method, as its maximum error is about 30% higher than the maximum error of CPD-ADI. This can be explained by the fact that more numerical approximations are used for the boundary conditions. However, we emphasize that the main feature of the new method is that it is capable of solving the homogeneous velocity problem. Given that these methods are fourth-order accurate, one can use a slightly finer grid to reach the same error level, with just a minor increase of computational time. One interesting observation is that the new method is highly consistent with CPD-ADI. This is true as the CPD-ADI method is equivalent to NCV-CPD-ADI method when they are used to solve constant-velocity problem, except for a minor difference on the approximation of the boundary conditions.

6. Conclusion and future work

A compact fourth-order ADI FD scheme has been developed in this paper to solve the two-dimensional acoustic wave equation in heterogeneous media. Due to the non-constant velocity, the existing compact higher-order ADI methods are not applicable to convert the original 2D problem into a sequence of 1D problems. We successfully resolved this issue by utilizing a novel algebraic manipulation on the difference operator. Theoretical analysis shows that the resultant method is fourth-order accurate in both time and space. The higher-order convergence order has been validated by two numerical examples for which the exact solutions are available. Moreover, we proved that the new method is conditionally stable. The stability condition is theoretically derived, then numerically validated using a numerical example. Numerical examples on a two-layer model shows that the new method is more accurate and less dispersive than the conventional second-order FD scheme. Numerical example also demonstrated that the new method is more robust, accurate and efficient than the existing typical FD schemes, and can be used for numerical seismic modeling on complex geological models such as the Marmousi model. In the future we plan to extend the method to three-dimensional problems and other more realistic boundary condition for instance the absorbing boundary condition. Also it will be an interesting work to extend the interlinked Padé approximation ADI method [6] to the non-constant velocity case, to further reduce numerical dispersion.

Acknowledgments

References

[1] A. Bayliss, K.E. Jordan, B. Lemesurier, E. Turkel, A fourth-order accurate finite difference scheme for the computation of elastic waves, Bull. Seismol. Soc. Am. 76 (4) (1986) 1115–1132.
[2] J.B. Chen, High-order time discretizations in seismic modelling, Geophysics 72 (2007) 115–122.
[3] P. Chu, C. Fan, A three-point combined compact difference scheme, J. Comput. Phys. 140 (1998) 370–399.
[4] G. Cohen, P. Joly, Construction and analysis of fourth-order finite difference schemes for the acoustic wave equation in non-homogeneous media, SIAM J. Numer. Anal. 4 (1996) 1266–1302.
[5] M.A. Dablain, The application of high-order differencing for the scalar wave equation, Geophysics 51 (1) (1986) 54–66.
[6] S. Das, W. Liao, A. Gupta, An efficient fourth-order low dispersive finite difference scheme for a 2-D acoustic wave equation, J. Comput. Appl. Math. 258 (2014) 151–167.
[7] J. Douglas Jr., J. Gunn, A general formulation of alternating direction methods part i. parabolic and hyperbolic problems, Numer. Math. 6 (1966) 428–453.
[8] G. Fairweather, A.R. Mitchell, A high accuracy alternating direction method for the wave equation, J. Inst. Math. Appl. 1 (1965) 309–316.
[9] B. Finkelstein, R. Kastner, Finite difference time domain dispersion reduction schemes, J. Comput. Phys. 221 (2007) 422–438.
[10] K.R. Kelly, R.W. Ward, S. Treitel, E.M. Alford, Synthetic seismograms: a finite difference approach, Geophysics 41 (1976) 2–27.
[11] S. Kim, H. Lim, High-order schemes for acoustic waveform simulation, Appl. Numer. Math. 57 (2007) 402–414.
[12] M. Lees, Alternating direction methods for hyperbolic differentials equations, J. Soc. Ind. Appl. Math. 10 (1962) 610–616.
[13] A.R. Levander, Fourth-order finite-difference P-SV seismograms, Geophysics 53 (11) (1988) 1425–1436.
[14] J. Li, M.R. Visbal, High-order compact schemes for nonlinear dispersive waves, J. Sci. Comput. 26 (1) (2006) 1–23.
[15] Z. Li, Compensating finite-difference errors in 3-D migration and modelling, Geophysics 56 (1991) 1650–1660.
[16] D. Ristow, T. Ruhl, 3-D implicit finite-difference migration by multiway splitting, Geophysics 62 (1997) 554–567.
[17] W. Liao, J. Zhu, A.Q. Khaliq, An efficient high-order algorithm for solving systems of reaction diffusion equations, Numer. Method Partial Differ. Eq. 18 (30) (2002) 340–354.
[18] W. Liao, On the dispersion, stability and accuracy of a compact higher-order finite difference scheme for 3D acoustic wave equation, J. Comput. Appl. Math. 270 (2014) 571–583.
[19] Y. Liu, M.K. Sen, An implicit staggered-grid finite-difference method for seismic modelling, Geophys. J. Int. 179 (2009a) 459–474.
[20] Y. Liu, M.K. Sen, A new time-space domain high-order finite-difference method for the acoustic wave equation, J. Comput. Phys. 228 (2009b) 8779–8806.
[21] B.G. Nita, Forward scattering series and padé approximants for acoustic wavefield propagation in a vertically varying medium, Commun. Comput. Phys. 3 (1) (2008) 180–202.
[22] G.W. Peaceman, H.H. Rachford, The numerical solution of parabolic and elliptic differential equations, J. Soc. Ind. Appl. Math. 3 (1) (1955) 28–41.
[23] G.R. Shubin, J.B. Bell, A modified equation approach to constructing fourth-order methods for acoustic wave propagation, SIAM J. Sci. Stat. Comput. 8 (2) (1987) 135–151.
[24] R. Shukla, X. Zhong, Derivation of high-order compact finite difference schemes for non-uniform grid using polynomial interpolation, J. Comput. Phys. 204 (2) (2005) 404–429.
[25] N. Takeuchi, R.J. Geller, Optimally accurate second order time-domain finite difference scheme for computing synthetic seismograms in 2-D and 3-D media, Phys. Earth Planet. Int. 119 (2000) 99–131.
[26] Y. Wang, J. Zhang, Sixth-order compact scheme combined with multi-grid method and extrapolation technique for 2D poisson equation, J. Comput. Phys. 228 (1) (2009) 137–146.
[27] D.H. Yang, J.M. Peng, M. Lu, T. Terlaky, Optimal nearly-analytic discrete approximation to the scalar wave equation, Bull. Seismol. Soc. Am. 96 (3) (2006) 1114–1130.
[28] D.H. Yang, N. Wang, S. Chen, G.J. Song, An explicit method based on the implicit Runge–Kutta algorithm for solving the wave equations, Bull. Seismol. Soc. Am.. 99 (6) (2009) 3340–3354.
[29] D.H. Yang, L. Wang, A split-step algorithm with effectively suppressing the numerical dispersion for 3D seismic propagation modeling, Bull. Seismol. Soc. Am. 100 (4) (2010) 1470–1484.
[30] D.H. Yang, et al., Simulation of acoustic wavefields in heterogeneous media: a robust method for automatic suppression of numerical dispersion, Geophysics 75.3 (2010) T99–T110.
[31] D.H. Yang, P. Tong, X.Y. Deng, A central difference method with low numerical dispersion for solving the scalar wave equation, Geophys. Prospect. 60 (5) (2012) 885–905.
[32] W. Zhang, L. Tong, E. Chung, A new high accuracy locally one-dimensional scheme for the wave equation, J. Comput. Appl. Math. 236.6 (2011) 1343–1353.